Acta Crystallographica Section F
Structural Biology and Crystallization Communications
ISSN 1744-3091

Purification and crystallization of RNase HIII from *Staphylococcus aureus*

Scott A. Reiling, Kohei Homma and Oluwatoyin A. Asojo*

Department of Pathology and Microbiology, College of Medicine, Nebraska Medical Center, Omaha, NE 68198-6495, USA

Correspondence e-mail: oasojo@unmc.edu

Received 9 September 2010
Accepted 6 November 2010

As part of collaborative efforts to characterize virulence factors from *Staphylococcus aureus*, methods for the large-scale recombinant production of RNase HIII from *S. aureus* subspecies MRSA252 (Sa-RNase HIII) have been developed. RNase HIII-type ribonucleases are poorly characterized members of the RNase H group of endonucleases which hydrolyze RNA from RNA/DNA hybrids and are thought to be involved in DNA replication and repair. They are characterized by N-terminal extensions of unknown function that do not share sequence homology with the N-terminal extensions of bacterial RNases HI and RNases HII. Sa-RNase HIII was crystallized in the orthorhombic space group $P2_12_12_1$, with unit-cell parameters $a = 48.9$, $b = 74.2$, $c = 127.5$ Å, and diffracted to 2.6 Å resolution.

1. Introduction

Methicillin-resistant *Staphylococcus aureus* (MRSA) is a major cause of nosocomially acquired infections, especially in immunocompromised individuals (Klein *et al.*, 2007). Community-acquired MRSA is also a health problem, especially among those of a poorer socioeconomic status (Klein *et al.*, 2007). There is a need for new approaches to drug development for MRSA. Virulence factors such as RNase HIII are potential candidates for rational drug design owing to their structural differences from host proteins; however, their structures remain undetermined. RNase HIII proteins belong to the type 2 RNase family (Chon *et al.*, 2005; Kochiwa *et al.*, 2007). RNase HIII has limited amino-acid sequence similarity to RNase HII, yet is part of the same family owing to mutually conserved sequence motifs (Chon *et al.*, 2004; Kochiwa *et al.*, 2007).

RNases hydrolyze RNA/DNA in the presence of various divalent cofactors such as Mg^{2+} and Mn^{2+} (Chon *et al.*, 2004) so as to eliminate RNA primers from Okazaki fragments during replication (Sato *et al.*, 2003). Structural similarity between interspecies homologs appears to be more important for function than sequence similarity; for example, the *Escherichia coli* RNases H share no more than 41% sequence homology with those of *Chlamydophila pneumoniae*, but RNases HII and HIII from *C. pneumoniae* can complement *E. coli* deficient in RNases HI and HII (Liang *et al.*, 2007). RNases HI and HII share a conserved sequence of four amino acids at the active site, consisting of Asp, Glu, Asp and Asp, while RNases HIII differ by an Asp/Glu substitution at the last residue (Chon *et al.*, 2006). The N-terminal domains of RNase H are known to have a substrate-binding capability that includes the aforementioned RNA/DNA hybrids and also dsDNA and dsRNA (Gaidamakov *et al.*, 2005). The biochemical and functional properties of the N-termini of RNases HI and HII have been studied extensively, whereas the large (70–90 amino-acid) N-terminal domain of RNase HIII remains largely unexamined. Recently, a study investigating the N-terminal extension of *Bacillus stearothermophilus* RNase HIII (Bst-RNase HIII) revealed that both the N-terminal domain alone and a deletion mutant could bind to

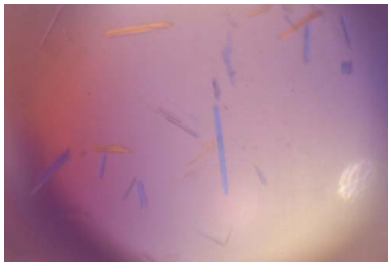

5′-GACGACGACAAGATG GAGAATCTTTATTTTCAGGGC TGGCGAATATCGTTTTTAAATTG-3′

Ek/LIC (FW) TEV protease recognition site sar1113

5′-GAGGAGAAGCCCGGTTA CAAAGAGGCTTTAAAATTTTTTG-3′

Ek/LIC (RV) sar1113

Figure 1
Primers used for PCR.

substrate, albeit with sevenfold and fivefold lower affinity compared with the wild type (Chon *et al.*, 2006). Additionally, Bst-RNase HIII offers the only three-dimensional structure of an RNase HIII (Chon *et al.*, 2006). There is a need to clarify the structure of RNase HIII in order to fully understand its substrate specificity. Despite their importance as potential drug targets, there is an absence of structural and biochemical data on *Staphylococcus aureus* RNases. To remedy this situation, and as part of efforts to characterize the structure and functions of virulence factors from *S. aureus*, we have expressed, purified and crystallized RNase HIII from *S. aureus* subspecies MRSA252 (Sa-RNase HIII) and present these preliminary studies here.

2. Materials and methods

2.1. Cloning and protein expression

Standard methods were employed for restriction-enzyme digestions, PCR, electrophoresis and heat-shock *E. coli* transformations (Sambrook *et al.*, 1989). The primers shown in Fig. 1 were used for PCR on genomic DNA generously provided by Dr Jeff Bose. The characteristic regions of each primer are labeled in Fig. 1 and include a TEV protease cleavage site. Sar1113 is the NCIBI nucleotide coding for Sa-RNase HIII from MRSA. The sar1113 predicted open reading frame (which encodes Sa-RNase HIII) was PCR-amplified and inserted into the ligation-independent cloning site of the pET-30 Ek/LIC plasmid (Novagen, Madison, Wisconsin, USA). Sequencing confirmed that this fused a hexahistidine tag to the N-terminus of each protein under the control of the plasmid's isopropyl β-D-1-thiogalactopyranoside (IPTG) inducible promoter and yields the expression construct pET30LICrnashiii. This construct has both an N-terminal hexahistidine tag and an S-tag, which are followed by a TEV protease-cleavage site (incorporated from the primer) to facilitate easy removal of the tags.

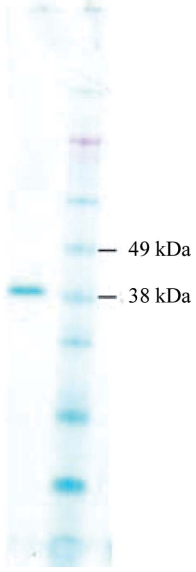

Figure 2
The sample used for crystallization was greater than 99% pure as assessed on a Coomassie-stained SDS–PAGE reduced gel and had a molecular mass close to the theoretical value of 35 kDa.

2.2. Protein expression

The construct pET30LICrnashiii was transformed into *E. coli* BL21 CodonPlus (DE3) RIPL Competent Cells (Stratagene) by heat shock and plated on solid Luria–Bertani (LB) medium containing chloramphenicol (35 µg l^{-1}) and kanamycin (50 µg l^{-1}). 25 ml of medium was inoculated with a single colony. The starter culture was grown at 310 K and 250 rev min^{-1} for 16 h. 1 l LB medium in a 2.8 l Fernbach flask was inoculated with the starter culture and allowed to grow at 310 K until the OD_{600} reached 0.5, at which point the culture was cooled to 291 K. Cells were grown at 291 K with shaking at 150 rev min^{-1} until the OD_{600} of the cells reached 0.8, at which point protein expression was induced by the addition of IPTG to a final concentration of 0.5 m*M*. Cells were grown for 6 h post-induction at 291 K with shaking at 225 rev min^{-1}. Each litre of culture was harvested by centrifugation at 8000*g* for 10 min at 277 K and frozen at 193 K until use.

2.3. Protein purification

Cell pellets harvested from a litre of culture were resuspended in 80 ml buffer *A* (300 m*M* NaCl, 50 m*M* Na_2HPO_4 pH 7.4) containing a Complete Mini EDTA-free protease-inhibitor tablet (Roche, Branford, Connecticut, USA) and 20 m*M* imidazole. Cells were ruptured by seven passes through an Emulsifex-C3 microfluidizer (Avestin Inc., Ottawa, Canada) at 103 MPa. Cellular debris was removed by centrifugation at 12 000*g* for 30 min. The supernatant was loaded onto a 5 ml Ni–NTA FF crude affinity column (GE Healthcare Biosciences; Piscataway, New Jersey, USA) using an ÄKTA FPLC high-performance liquid-chromatography system (GE Healthcare Biosciences). Rnase HIII was eluted in a single peak with a linear imidazole gradient (150–250 m*M*) in buffer *A*. Typically, each litre of culture yielded at least 150 mg soluble protein with a purity greater than 95% at this stage. The protein was dialyzed into buffer *A* to remove imidazole prior to removal of the affinity tags. The affinity tags were cleaved by incubation with recombinant polyhistidine-tagged S219V mutant tobacco etch virus (TEV) protease in buffer *A* for 24 h at 277 K followed by 1 h incubation at 310 K. The ratio (in milligrams) of Sa-RNase HIII to TEV protease was 1:3 as assessed by OD_{280}. Uncleaved Sa-RNase HIII and TEV protease were removed by subsequent Co-chelating chromatography using buffer *A*, yielding at least 99% pure Sa-RNase HIII as assessed by Coomassie-stained SDS–PAGE (Fig. 2). The final yield from each litre of culture was typically 50 mg untagged Sa-RNase HIII. The resulting protein has an additional Gly residue at the N-terminus, which is a remnant of the TEV protease recognition site. TEV protease was produced from

Addgene plasmid 8827 (Kapust *et al.*, 2001) according to the manufacturer's instructions.

2.4. Crystallization

Initial crystallization screens were carried out on samples of His-tagged Sa-RNase HIII using sparse-matrix screens from both Qiagen (Cryo, Classics, Classics II, JCSG+, $AmSO_4$ and MPD Suites) and Hampton Research (Crystal Screen Cryo, Crystal Screen and Crystal Screen 2). Despite screening at various temperatures and with protein concentrations between 10 and 50 mg ml^{-1} in various buffers at pH values ranging from 4.5 (acetate) to 8.5 (Tris–HCl), no hits were obtained; consequently, the protein was TEV-cleaved to remove the His tag and the screening was repeated. After screening only 50 conditions of Hampton Crystal Screen Cryo, preliminary crystals of Sa-RNase HIII were obtained. These crystals grew by vapor diffusion in sitting drops using a VDX plate at 293 K (Hampton Research) containing 0.45 ml crystallization solution in the reservoir. Drops were prepared by mixing 4 µl protein solution with 2 µl crystallization solution. The protein solution for crystallization experiments consisted of 3.2 mg ml^{-1} Sa-RNase HIII in PBS (137 m*M* NaCl, 2.7 m*M* KCl, 10 m*M* sodium phosphate dibasic, 2 m*M* potassium phosphate monobasic pH 7.4). The initial protein concentration was confirmed spectrophotometrically prior to setting up crystallization experiments using a NanoDrop ND1000 (Thermo Fisher). The largest crystals were obtained within 48 h from a precipitant solution comprised of 0.17 *M* ammonium sulfate, 25.5%(*w*/*v*) PEG 8000, 15%(*v*/*v*) glycerol and 0.085 *M* sodium cacodylate pH 6.5. These plate-like rod crystals were less than 0.02 mm in the smallest dimension despite being over 0.3 mm in the largest dimension (Fig. 3).

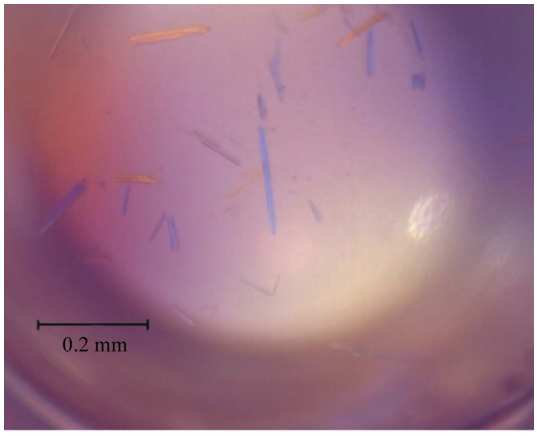

(*a*)

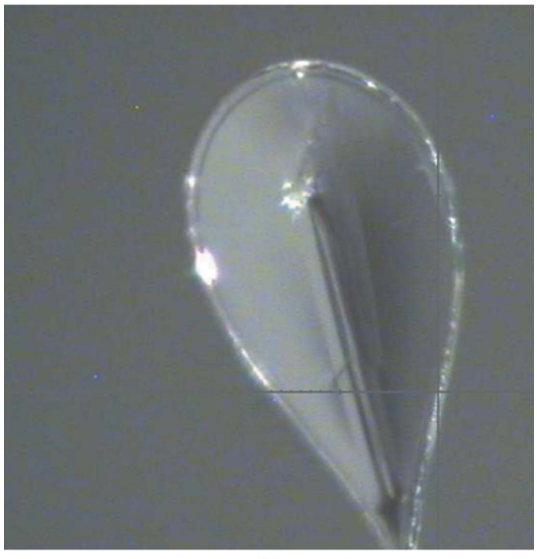

(*b*)

Figure 3
(*a*) Needle-like plate crystals were obtained directly from Hampton Research Crystal Screen Cryo condition No. 15. (*b*) The largest crystal is approximately 0.2 mm on the longest side and less than 0.02 mm on the smallest side and is shown mounted in a 0.2–0.3 mm loop.

Table 1
Data-collection and reduction statistics.

Values in parentheses are for the highest resolution shell.

Low-resolution limit (Å)	28.72 (2.70)
High-resolution limit (Å)	2.59 (2.59)
$R_{\rm merge}$† (%)	10.0 (38.8)
Total No. of observations	52706 (4766)
Total No. of unique reflections	26458 (2653)
Mean $I/\sigma(I)$	7.34 (1.31)
Completeness (%)	94.6 (66.6)
Multiplicity	3.4 (3.3)

† $R_{\rm merge} = \sum_{hkl}\sum_i |I_i(hkl) - \langle I(hkl)\rangle| / \sum_{hkl}\sum_i I_i(hkl)$, where $I_i(hkl)$ and $\langle I(hkl)\rangle$ are the intensity of the ith measurement and the mean intensity of the reflection with indices hkl, respectively.

2.5. Diffraction experiments

Since the crystals were grown in a cryoprotecting solution, they were flash-cooled in a stream of N_2 gas at 100 K immediately prior to collecting diffraction data. Data sets were collected in-house using a four-circle kappa platform Xcalibur PX Ultra with a 165 mm diagonal Onyx CCD detector and a high-brilliance sealed-tube Cu Enhance Ultra X-ray source (Oxford Diffraction, Oxford, England) operating at 50 kV and 40 mA. The diffraction pattern confirmed that the crystal was indeed of protein and not salt (Fig. 4). Initial data sets for each crystal were collected from single crystals using a crystal-to-

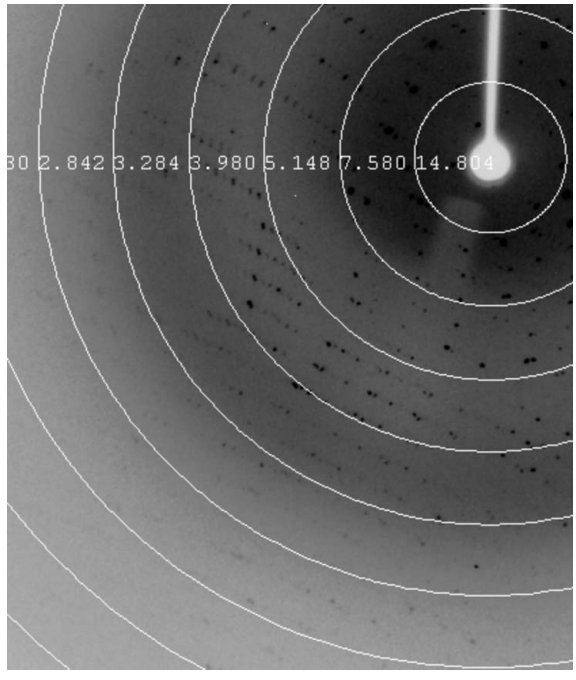

Figure 4
The crystal has visible diffraction spots to about 2.6 Å resolution and the diffraction pattern is as expected for a protein, not a salt.

detector distance of 65 mm and an exposure time of 100 s per 0.5° oscillation. X-ray data were processed using the program *Crysalis*^{Pro} (Oxford Diffraction). The crystal belonged to space group $P2_12_12_1$, with unit-cell parameters a = 48.9, b = 74.2, c = 127.5 Å. Crystallographic data are given in Table 1. Based on the estimated Matthews probability and solvent-content prediction (http://www.ruppweb.org/Mattprob), we expect a monomer in the asymmetric unit (Matthews, 1968; Kantardjieff & Rupp, 2003). This corresponds to 64% solvent content or a Matthews coefficient of 3.43 Å^3 Da^{-1}.

3. Results and discussion

We have successfully cloned, expressed and purified Sa-RNase HIII and identified crystallization conditions in the orthorhombic space group $P2_12_12_1$. Crystals could only be obtained after removal of the N-terminal hexahistidine tag. Sample crystals permitted the collection of data to 2.6 Å resolution in the home laboratory. Attempts at phasing by maximum-likelihood methods with the program *Phaser* (McCoy *et al*., 2005; Storoni *et al.*, 2004) using a polyalanine model of Bst-RNase HIII (PDB code 2doa; Chon *et al.*, 2006) as the search model gave a solution with an initial R factor of 45% (free R factor of 49%). The model was submitted to automatic model-building programs such as *Buccaneer* (Cowtan, 2006) and *ARP*/*wARP* (Morris *et al.*, 2003); despite successful rebuilding of the entire coordinates, neither the R factor nor the free R factor dropped appreciably and the resulting electron-density maps were choppy. The anisotropy diffraction server (http://people.mbi.ucla.edu/sawaya/anisoscale/) was used to analyze our data set and indicated severe anisotropy, with only 3.2 Å quality in one direction; this could account for the stalled refinement. Future efforts include improving the quality of the crystals in order to generate better quality data. We hope that determination of this structure will aid in the identification of unique motifs that will facilitate the development of this family of proteins as potential drug targets.

Thanks to Dr Jeff Bose for his generous gift of *S. aureus* subspecies MRSA252 genomic DNA. Thanks to Dr Paul Dunman for introducing us to RNases and identifying the sar1113 ORF.

References

Chon, H., Matsumura, H., Koga, Y., Takano, K. & Kanaya, S. (2005). *Acta Cryst.* F**61**, 293–295.
Chon, H., Matsumura, H., Koga, Y., Takano, K. & Kanaya, S. (2006). *J. Mol. Biol.* **356**, 165–178.
Chon, H., Nakano, R., Ohtani, N., Haruki, M., Takano, K., Morikawa, M. & Kanaya, S. (2004). *Biosci. Biotechnol. Biochem.* **68**, 2138–2147.
Cowtan, K. (2006). *Acta Cryst.* D**62**, 1002–1011.
Gaidamakov, S. A., Gorshkova, I. I., Schuck, P., Steinbach, P. J., Yamada, H., Crouch, R. J. & Cerritelli, S. M. (2005). *Nucleic Acids Res.* **33**, 2166–2175.
Kantardjieff, K. A. & Rupp, B. (2003). *Protein Sci.* **12**, 1865–1871.
Kapust, R. B., Tözsér, J., Fox, J. D., Anderson, D. E., Cherry, S., Copeland, T. D. & Waugh, D. S. (2001). *Protein Eng.* **14**, 993–1000.
Klein, E., Smith, D. L. & Laxminarayan, R. (2007). *Emerg. Infect. Dis.* **13**, 1840–1846.
Kochiwa, H., Tomita, M. & Kanai, A. (2007). *BMC Evol. Biol.* **7**, 128.
Liang, R., Liu, X., Pei, D. & Liu, J. (2007). *Microbiology*, **153**, 787–793.
Matthews, B. W. (1968). *J. Mol. Biol.* **33**, 491–497.
McCoy, A. J., Grosse-Kunstleve, R. W., Storoni, L. C. & Read, R. J. (2005). *Acta Cryst.* D**61**, 458–464.
Morris, R. J., Perrakis, A. & Lamzin, V. S. (2003). *Methods Enzymol.* **374**, 229–244.
Sambrook, J., Fritsch, E. F. & Maniatis, T. (1989). *Molecular Cloning: A Laboratory Manual*, 2nd ed. New York: Cold Spring Harbor Laboratory Press.
Sato, A., Kanai, A., Itaya, M. & Tomita, M. (2003). *Biochem. Biophys. Res. Commun.* **309**, 247–252.
Storoni, L. C., McCoy, A. J. & Read, R. J. (2004). *Acta Cryst.* D**60**, 432–438.